

Yeast AEP3p Is an Accessory Factor in Initiation of Mitochondrial Translation*

Received for publication, August 13, 2009, and in revised form, October 19, 2009. Published, JBC Papers in Press, October 20, 2009, DOI 10.1074/jbc.M109.055350

Changkeun Lee¹, Anne S. Tibbetts, Gisela Kramer, and Dean R. Appling²

From the Department of Chemistry and Biochemistry and the Institute for Cellular and Molecular Biology, The University of Texas, Austin, Texas 78712

Initiation of protein synthesis in mitochondria and chloroplasts normally uses a formylated initiator methionyl-tRNA (fMet-tRNA_f^{Met}). However, mitochondrial protein synthesis in *Saccharomyces cerevisiae* can initiate with nonformylated Met-tRNA_f^{Met}, as demonstrated in yeast mutants in which the nuclear gene encoding mitochondrial methionyl-tRNA formyltransferase (*FMT1*) has been deleted. The role of formylation of the initiator tRNA is not known, but *in vitro* formylation increases binding of Met-tRNA_f^{Met} to translation initiation factor 2 (IF2). We hypothesize the existence of an accessory factor that assists mitochondrial IF2 (mIF2) in utilizing unformylated Met-tRNA_f^{Met}. This accessory factor might be unnecessary when formylated Met-tRNA_f^{Met} is present but becomes essential when only the unformylated species are available. Using a synthetic petite genetic screen in yeast, we identified a mutation in the *AEP3* gene that caused a synthetic respiratory-defective phenotype together with Δ *fnt1*. The same *aep3* mutation also caused a synthetic respiratory defect in cells lacking formylated Met-tRNA_f^{Met} due to loss of the *MIS1* gene that encodes the mitochondrial C₁-tetrahydrofolate synthase. The *AEP3* gene encodes a peripheral mitochondrial inner membrane protein that stabilizes mitochondrially encoded *ATP6/8* mRNA. Here we show that the *AEP3* protein (Aep3p) physically interacts with yeast mIF2 both *in vitro* and *in vivo* and promotes the binding of unformylated initiator tRNA to yeast mIF2. We propose that Aep3p functions as an accessory initiation factor in mitochondrial protein synthesis.

Initiation factor 2 (IF2)³ plays a critical role in the initiation of translation. IF2 binds the initiator tRNA, then positions it over the initiation codon of the mRNA on the ribosome in a GTP-dependent process (1). IF2 is conserved in bacteria and mitochondria (2) and is assumed to have a native structure similar to the cytoplasmic initiation factor eIF5B found in Archaea and

eukaryotes (3). Bacterial and mitochondrial IF2s share similar domain structures and biochemical properties (4–9).

In eubacteria, the initiator Met-tRNA_f^{Met} is formylated by the enzyme methionyl-tRNA formyltransferase. Formylated methionyl-tRNA (fMet-tRNA_f^{Met}), along with Met-tRNA formyltransferase activity, is also observed in mitochondria of eukaryotes such as *Saccharomyces cerevisiae*, *Neurospora crassa*, and mammals (10–13). These observations along with the identification of formylmethionine at the N terminus of several mitochondrially synthesized proteins (14) led to the widely accepted dogma that mitochondrial protein synthesis initiation requires fMet-tRNA_f^{Met} in a process involving mitochondrial IF2. However, it is now recognized that, at least in *S. cerevisiae*, mitochondrial protein synthesis can initiate with non-formylated Met-tRNA_f^{Met}, as demonstrated in yeast mutants in which the nuclear gene for mitochondrial Met-tRNA_f^{Met} transformylase (*FMT1*) has been deleted (15, 16).

Mitochondrial IF2 (mIF2) is the only initiation factor thus far identified for the yeast mitochondrial system. Three proteins (IF1, IF2, and IF3) are essential for initiation in eubacteria (17), and there must certainly be additional factors involved in initiation of mitochondrial protein synthesis. Koc and Spremulli (18) have characterized a mammalian mitochondrial IF3, but no IF3 homolog has been found in the *S. cerevisiae* genome. Mammalian mIF3 promotes initiation complex formation on mitochondrial ribosomes and promotes ribosome dissociation (18), like its bacterial IF3 counterpart. A possible yeast homolog was suggested by BLAST analysis, but this gene (YGL159w) is not required for mitochondrial respiration (19) and is, thus, not likely to encode the yeast mitochondrial IF3. IF1 homologs are present in all three domains of life (bacteria, Archaea, eukaryotes) (20), but no IF1 homolog has been detected in any mitochondrial translation system. Instead, biochemical and molecular modeling studies suggest that mammalian mIF2 may perform the functions of both IF2 and IF1 (21).

Mammalian mIF2 is reported to be 20–50-fold more active with formylated *versus* non-formylated Met-tRNA_f^{Met} *in vitro* (22). Yeast mIF2 (ymIF2) is also more active with the formylated initiator tRNA *in vitro* but has an enhanced ability to bind unformylated initiator Met-tRNA relative to the bovine protein (8, 9). Yet both of these mIF2s support translation initiation *in vivo* with unformylated Met-tRNA_f^{Met} (16). Based on these observations, we hypothesize the existence of an accessory factor that assists mIF2 in utilizing unformylated Met-tRNA_f^{Met}. This accessory factor might be unnecessary when formylated Met-tRNA_f^{Met} is present but becomes essential when only the unformylated species is available.

* This work was supported by United States Army Research Office Grant W911NF-07-1-0040.

¹ Present address: Dept. of Physiology, University of Texas Southwestern Medical Center, 5323 Harry Hines Blvd., Dallas, TX 75390-9040.

² To whom correspondence should be addressed: Dept. of Chemistry and Biochemistry, The University of Texas at Austin, 1 University Station A5300, Austin TX 78712-0165. Tel.: 512-471-5842; Fax: 512-471-5849; E-mail: dappling@mail.utexas.edu.

³ The abbreviations used are: IF2, initiation factor 2; mIF2, mitochondrial IF2; ymIF2, yeast mIF2; Aep3p, protein encoded by *AEP3* gene; 5-FOA, 5-fluoroorotic acid; MBP, maltose-binding protein; MBP-Aep3, MBP-Aep3 fusion protein; ORF, open reading frame; PPR, pentatricopeptide repeat; UTR, untranslated region; fMet-tRNA_f^{Met}, formylated methionyl-tRNA; THF, tetrahydrofolate; s.p., synthetic petite strain; HA, hemagglutinin.

To search for other factors potentially involved in the initiation of mitochondrial protein synthesis, we developed a genetic screen using a strain ($\Delta fmt1$) lacking formylated initiator tRNA (15). Mitochondrial protein synthesis is required for respiratory function in mitochondria, and mutation of genes encoding mitochondrial translation components invariably leads to a respiratory-deficient (petite) phenotype (23). Thus, the screen was designed to identify mutants that cause a respiratory defect only in combination with the $\Delta fmt1$ mutation (*i.e.* synthetic petites). One of the genes identified in this screen (*AEP3*) encodes a peripheral mitochondrial inner membrane protein reported to stabilize the bicistronic transcript of the mitochondrially encoded *ATP6* and *ATP8* genes (24). Here we show that the *AEP3* protein (Aep3p) physically interacts with ymIF2 and promotes the binding of unformylated initiator tRNA to ymIF2.

EXPERIMENTAL PROCEDURES

Chemicals, Reagents, and Strains—*Escherichia coli* tRNAs (tRNA_f^{Met} and tRNA^{Lys}) and cycloheximide were purchased from Sigma. Isopropyl- β -D-thiogalactopyranoside was purchased from Ambion (Austin, TX). NTA-matrix (HisBind resin) and KOD Hot Start DNA polymerase were from Novagen (Gibbstown, NJ). Restriction enzymes were purchased from either Invitrogen or Fisher/Promega (Madison, WI). Oligonucleotides were synthesized by IDT (Coralville, IA) or BioSynthesis (Lewisville, TX). Geneticin (G-418 sulfate) was obtained from American Bioanalytical (Natick, MA). Kits for plasmid preparation or for extraction of DNA were from Qiagen (Valencia, CA). [³⁵S]Methionine and [¹⁴C]lysine were purchased from PerkinElmer Life Sciences.

The aminoacylation and formylation of *E. coli* initiator tRNA_f^{Met} with [³⁵S]Met has been described in detail previously (8). Both Met-tRNA_f^{Met} and fMet-tRNA_f^{Met} were prepared in parallel using the same batch of *E. coli* tRNA and the same specific radioactivity of [³⁵S]Met (~10,000 Ci/mol). tRNA^{Lys} was aminoacylated with [¹⁴C]Lys (~300 Ci/mol) by the same procedure used to prepare [³⁵S]Met-tRNA_f^{Met}.

S. cerevisiae strains and plasmids are listed in Table 1. Yeast cells were grown in YPD (1% yeast extract, 2% Bacto-peptone, and 2% glucose), YPEG (1% yeast extract, 2% Bacto-peptone, 2% ethanol, and 3% glycerol), or YMD (0.7% yeast nitrogen base without amino acids, 2% glucose) as described previously (16). Plates used for eviction of *URA3* plasmids contained 0.1% 5-FOA (Biovectra; Charlottetown, PEI, Canada). Yeast genomic DNA was isolated using the Qiagen DNeasy Blood and Tissue kit. Haploid $\Delta aep3$ cells (DLY2) were generated from EUROSCARF strain Y22823 (Table 1) by sporulation and tetrad dissection as described previously (25). DLY2 was maintained with a plasmid (pRS416-AEP3, Table 1) encoding the wild-type *AEP3* gene, as *aep3* deletion mutants are respiratory-deficient (petite) and exhibit mitochondrial DNA instability (24). Other *AEP3* constructs could then be transformed into DLY2 on pRS415 and studied after eviction of the wild-type pRS416-AEP3 plasmid by growth on 5-FOA.

Full-length ymIF2 as well as the C2-subdomain of ymIF2 were prepared as described previously (8, 9). Yeast cytoplasmic C₁-THF synthase was purified as described (26).

Polyclonal antibodies against purified recombinant His-tagged ymIF2 were produced in rabbits by the MD Anderson Cancer Center (Bastrop, TX). The IgG-fraction of the immune serum was purified by Protein A-Sepharose (Sigma) chromatography. This IgG fraction was used in the experiments described below.

Genetic Screen for Mutations Creating a Synthetic Petite Phenotype in the Presence of $\Delta fmt1$ —The *FMT1* gene, including 360 bp of upstream sequence, was PCR-amplified from DAY4 yeast genomic DNA (using oligonucleotides FMT1f2 (5'-CAGTGGATCCACACCCAATTGCGAGCC-TAA-3') and FMT1r2 (5'-GTAGATCGATATGTAGAGCC-GGGTTACAGG-3'), cleaved with BamHI and ClaI, and ligated into the centromeric shuttle vector, pRS416. The Y03039 ($\Delta fmt1$) strain was transformed with the resulting pRS416-FMT1 construct, selecting for Ura⁺ transformants. The resulting strain was grown in minimal media to late log phase and exposed to UV mutagenesis in a Stratalinker UV cross-linker for 6 s, resulting in ~20% cell survival. Mutagenized cells were diluted and plated for single colonies on YPEG (rich complete, nonfermentable) medium and incubated at 30 °C for 6–7 days. Colonies were replica-plated from the YPEG plates onto minimal glucose media (YMD) containing 1 g/liter 5-FOA and amino acids necessary for Y03039 growth. After the forced eviction of the pRS416-FMT1 plasmid, colonies from the YMD/5-FOA plates were replica-plated once again onto YPEG medium. Approximately 10,000 colonies were screened (200 plates with ~50 colonies/plate), and mutants able to grow on the first YPEG plate (with the wild-type *FMT1* gene on a plasmid) but unable to grow on the second YPEG plate (after plasmid eviction) were isolated. The synthetic petite phenotype was verified by re-streaking the cells on the same series of plates. Putative synthetic petite mutants were crossed with a $\Delta fmt1$ strain of opposite mating type, and resulting diploids were spread onto YPEG/5-FOA plates, testing for the presence of a recessive nuclear mutation responsible for the synthetic petite phenotype. Eight synthetic petite strains were isolated from the screen; the synthetic petite strain 175 (s.p. 175) was used for the studies reported herein.

Isolation and Identification of the Genes Complementing the s.p. 175 Mutation—The s.p. 175 strain transformed with pRS416-FMT1 was transformed with a yeast genomic DNA library in the *LEU2* plasmid p366 (ATCC #77162) using the 10 \times yeast transformation protocol from Gietz and Woods (27). Transformants (~6000) were replica-plated onto YPEG/5-FOA, testing for complementation of respiratory growth by a library plasmid. Genomic library plasmid DNA was rescued (28) from the cells that grew robustly on YPEG/5-FOA and transformed into electrocompetent *E. coli* for plasmid preparation. Yeast genomic DNA was sequenced from these constructs using p366 plasmid-specific primers, p366s1 (5'-GCTACTTG-GAGCCACTATCGACTAC-3') and p366s3 (5'-CAGCAAC-CGCACCTGTGG-3'). The wild-type *AEP3* gene was PCR-amplified from DAY4 genomic DNA using primers A3_FOR (5'-AGCCTCGAGCCATAGCAGATTATACTA-3' (the XhoI site is underlined)) and A3_REV (5'-AATGGATCCTTCCTGTCC-AAATGC-3' (the BamHI site is underlined)), cleaved with BamHI and XhoI, and ligated into pRS416 and pRS415.

AEP3p Functions in Mitochondrial Translation Initiation

Disruption of *MIS1* in the *aep3-Y305N* Synthetic Petite Strain—Oligonucleotide primers with the *MIS1* flanking sequence on the 5' ends (forward primer, 5'-**CATTTGTCAGATATTTA-AGGCTAAAAGGAAATGTTGTTCGATCGAGGAGAACT-TCTAGTA**-3'; reverse primer, 5'-**TGCAGACGGACATCG-AGGTCGAATTGATGCCATTAGGAGTTCGCTCTACCC-TATGAACAT**-3'; *MIS1* sequences are in bold) were used to PCR-amplify the *LEU2* locus from pRS415 plasmid DNA. The resulting fragment was transformed into the s.p. 175 strain already harboring the pRS416-FMT1 plasmid, selecting for Leu⁺ Ura⁺ transformants. Yeast genomic DNA was isolated from Leu⁺ Ura⁺ strains, and PCR (forward primer, 5'-GCT-AAAAGGAAATGTTGTTCG-3'; reverse primer, 5'-CATCGA-GGTCGAATTGATGC-3') was performed to confirm the disruption of the *MIS1* locus ($\Delta mis1::LEU2$) in the resulting strain (ATY6, Table 1). As predicted, the *MIS1* primers gave a 3-kbp product for the wild-type *MIS1* locus and a 1.85-kbp product for the disrupted locus ($\Delta mis1::LEU2$).

Cloning Yeast AEP3 for Protein Expression in *E. coli*—The wild-type *AEP3* ORF (YPL005W) was amplified from genomic DAY4 DNA using primers AP3-pMAL-For (5'-CCGGGATC-CATGAATACATTAAGG-3'; the BamHI site is underlined, and the start codon is in bold) and AP3-pMAL-Rev (5'-CCG-AAGCTTCAAACCTCCCCAAC-3'; the HindIII site is underlined, and the stop codon is in bold). PCR was carried out using KOD Hot Start DNA polymerase. The resulting PCR fragment was digested with BamHI and HindIII, gel-purified, inserted behind the maltose-binding protein (MBP) ORF of pMALc2H₁₀T (a gift from Dr. John Tesmer, University of Michigan) (29), and transformed into *E. coli* JM109 to generate MBP-Aep3p. The construct was verified by sequencing at the DNA Core Facilities of the Institute for Cellular and Molecular Biology at the University of Texas at Austin. Recombinant plasmid was transformed into *E. coli* Rosetta(DE3) cells (Novagen) to express the MBP and decahistidine tag fused to the full-length Aep3 protein (MBP-Aep3). Heterologous protein was expressed by growth in Luria broth and induction with 0.1 mM isopropyl- β -D-thiogalactopyranoside at 15 °C overnight. The cells were harvested, washed, and stored at -80 °C.

Purification of MBP-Aep3—Cells from a 2-liter culture of *E. coli* expressing MBP-Aep3 were lysed by sonication in 50 ml of 1× binding buffer (5 mM imidazole, 20 mM Tris-HCl, pH 7.9, 500 mM NaCl) to which one tablet of protease inhibitor (Roche Applied Science) was added. Cells were lysed by sonication on ice (15 s with 15-s intervals for 6 cycles). The supernatant was collected after centrifugation at 17,000 rpm for 30 min and applied to a 5-ml His-Bind column that had been charged with Ni²⁺ and equilibrated in 1× binding buffer. After washing with 50 ml of binding buffer, loosely bound protein was eluted with wash buffer containing 60 mM imidazole, 500 mM NaCl in Tris buffer. Tightly bound protein was eluted by 250 mM imidazole in the same Tris/NaCl buffer. The pooled protein fractions were dialyzed against 500 ml of 20 mM Tris-HCl, pH 7.5, for 4 h and stored at -80 °C in small aliquots. Protein concentration was determined by the Bradford assay (30), and purity was analyzed by SDS-PAGE (31). The maltose-binding protein alone was expressed from pMALc2H₁₀T and purified as described above to serve as a control in the binding assays.

In Vitro Filter Binding Assay—The filter binding assay described by Sundari *et al.* (32) was used to study tRNA binding to yeast ymIF2 and MBP-Aep3. Different amounts of each protein were incubated for 20 min on ice in 50 μ l of total volume containing 50 mM Tris-HCl, pH 7.0, 2 mM dithiothreitol, and 10 μ g of bovine serum albumin with 4 pmol of ³⁵S-labeled initiator tRNA (fMet-tRNA^{Met} or Met-tRNA^{Met}). [¹⁴C]Lys-tRNA^{Lys} and MBP were used in control reactions. Binding reactions were stopped with 2 ml of ice-cold solution containing 50 mM Tris-HCl, pH 7.0, and 2 mM dithiothreitol and then filtered through nitrocellulose filters followed by washing 5 times with the same buffer. Filters were dried, and radioactivity on filters was determined by liquid scintillation counting. Each assay was performed in duplicate.

MBP Pulldown Assay—MBP-Aep3 and ymIF2 (concentrations indicated in the legends to Figs. 3, 4, and 6) were incubated at room temperature with gentle rotation for 2 h in 200- μ l final volume containing 20 mM Tris-HCl, pH 7.4, 150 mM NaCl, 5 mM EDTA, 2 mM dithiothreitol. Thirty μ l of a slurry containing amylose affinity beads (New England Biolabs; diluted 50% with phosphate-buffered saline) were added and incubated for an additional 1 h while rotating at room temperature. The beads were spun down and removed from the supernatant (unbound fraction) and then washed six times using the same buffer. Bound proteins were eluted from the washed beads by boiling for 5 min in SDS-PAGE sample buffer and analyzed by SDS-PAGE on 10% gels. MBP alone and yeast cytoplasmic C₁-THF synthase were used as control proteins. Immunoblotting was performed using antibodies against ymIF2 or yeast cytoplasmic C₁-THF synthase (33). The immunoblots were visualized with the enhanced chemiluminescence detection system (GE Healthcare).

In Vivo Co-immunoprecipitation—An epitope-tagged version of *AEP3* with the hemagglutinin (HA) epitope fused to its C terminus was constructed by PCR amplification of the *AEP3* gene using forward primer A3-FOR (5'-AGCCTCGAGCAT-AGCAGATTATACTA-3'; the XhoI site is underlined) and reverse primer AP3-HA-Rev (5'-GGCGGATCCTCAAGC-GTAGTCTGGGACGTCGTATGGGTAACCTCCCCAAC-TATTCTCTCTTTAC-3'; the BamHI site is underlined, and the stop codon is in bold; HA epitope tag sequence italicized). The resulting PCR product was digested with XhoI and BamHI, gel-purified, and ligated into pRS415. The resulting construct (pRS415-AEP3-HA) was sequence-verified.

Yeast cells containing HA-tagged *AEP3* were grown in YMD, harvested, and washed twice with ice-cold water. Cells were resuspended in 500 μ l of co-immunoprecipitation buffer (34) containing 50 mM Tris-HCl, pH 7.5, 100 mM NaCl, 10% glycerol, 1 mM dithiothreitol, 10 mM MgCl₂, and one complete-mini EDTA-free protease inhibitor mixture tablet. Cells were disrupted with glass beads using a FastPrep FP120 cell disrupter (Qbiogene). A cleared soluble lysate was obtained by centrifugation at 16,000 rpm for 30 min. This was saved, and the glass beads were washed in 500 μ l of same buffer and centrifuged again. The two supernatants were combined (1 ml total) and then incubated with 10 μ l of anti-HA antibodies (1:100 dilution; Covance, Trenton, NJ) at 4 °C for 4 h with gentle rotation.

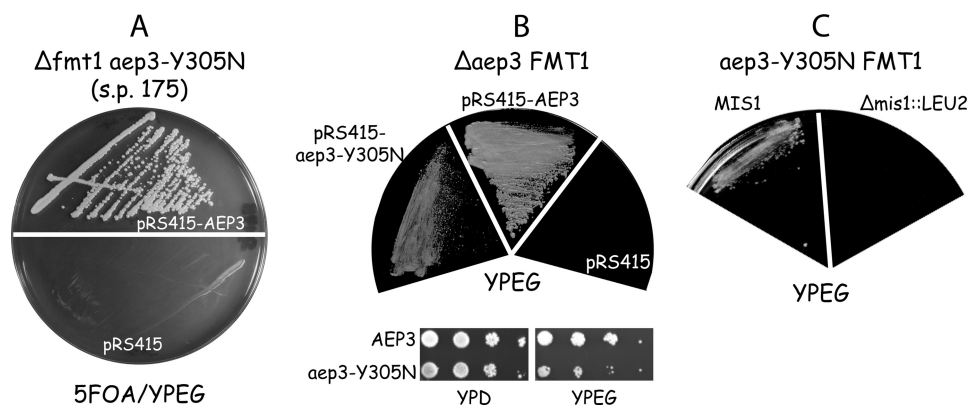


FIGURE 1. Point mutation in *AEP3* causes a synthetic respiratory defect in strains lacking formylated Met-tRNA^{Met}. *A*, synthetic petite mutant strain 175 ($\Delta fnt1$ *aep3*-Y305N), harboring full-length *FMT1* on a *URA3* plasmid, was transformed with either wild-type pRS415-*AEP3* (top) or empty plasmid (pRS415, bottom) as a negative control, streaked onto a 5-FOA/YPEG plate, and incubated at 30 °C for 5 days. *B* (top), strain DLY2 ($\Delta aep3$ *FMT1*⁺), harboring wild-type *AEP3* on a *URA3* plasmid (pRS416), was transformed to leucine prototrophy with either pRS415-*aep3*-Y305N, wild-type pRS415-*AEP3*, or empty plasmid (pRS415) as a negative control. The pRS416-*AEP3* plasmid was evicted by growth on 5-FOA, and then the transformants were streaked onto a YPEG plate and incubated at 30 °C for 5 days. *Bottom*, 10-fold serial dilutions of DLY2 harboring either the wild-type or mutant *aep3* plasmid were spotted on YPD or YPEG plates and incubated at 30 °C for 3 or 6 days, respectively. *C*, the original synthetic petite 175 strain ($\Delta fnt1$ *aep3*-Y305N *leu2* *MIS1*/pRS416-*FMT1*) and a Leu⁺ integrant of this strain were streaked onto YPEG plates and incubated at 30 °C for 5 days to test for respiratory growth. *MIS1*, wild-type *MIS1* locus, $\Delta mis1::LEU2$, disrupted *mis1* locus. See "Experimental Procedures" for details of *MIS1* gene disruption.

Fifty μ l of Protein A-Sepharose beads (Invitrogen) was then added, and the incubation was continued at 4 °C overnight. Immunocomplexes were collected by centrifugation at 1500 rpm for 2 min, washed 5 times with 500 μ l of co-immunoprecipitation buffer, and eluted from the beads with 50 μ l of SDS-PAGE sample buffer. Five μ l of each immunoprecipitate were analyzed by SDS-PAGE on a 10% gel followed by immunoblotting with the ymIF2 polyclonal antibody (1:10,000 dilution).

Labeling of Mitochondrial Translation Products—Yeast cells were inoculated in 10 ml of synthetic complete medium (0.7% yeast nitrogen base and standard concentrations of adenine, uracil, and amino acids) (35) containing 2% (w/v) galactose as the carbon source. Leucine was omitted from the synthetic complete-galactose medium for growth of the DLY2 strains transformed with *LEU2* plasmids (pRS415-*AEP3* and pRS415-*aep3*-Y305N), and uracil was omitted for growth of strain s.p. 175 harboring the pRS416-*FMT1* plasmid. In some experiments Ura⁺ plasmids (pRS416-*FMT1* or pRS416-*AEP3*) were evicted from *AEP3* mutant strains by streaking on YMD/5-FOA plates before metabolic labeling. Cells were grown to mid-log phase, harvested, and washed with minimal galactose medium (0.7% yeast nitrogen base, 2% galactose) without amino acids. *In vivo* labeling of mitochondrial translation products using [³⁵S]methionine in the presence of cytoplasmic protein synthesis inhibitor cycloheximide was performed as described previously (36). Translation products were separated by SDS-PAGE using gels (15% acrylamide, 0.1% bisacrylamide) prepared as described (36). Typically, 25% of the final resuspended protein extract was loaded on the gel for SDS-PAGE analysis.

Yeast strains used in these metabolic labeling experiments were also tested for respiratory deficiency using a tetrazolium overlay assay (15, 37). Cells grown in synthetic complete-galactose medium were plated on rich glucose me-

dium, and colonies were covered with agar containing 0.1% 2,3,5-triphenyltetrazolium chloride to determine the number of respiratory-defective (petite; white) and respiratory-competent (red) colonies.

RESULTS

Isolation of Mutants That Are Synthetically Petite with $\Delta fnt1$ —Deletion of the *FMT1* gene has no effect on respiratory growth (15). Because the only phenotype of a $\Delta fnt1$ mutant is the lack of formylated initiator tRNA (15), we reasoned that genes identified in this screen would likely encode proteins specifically involved in the initiation process of mitochondrial translation. The genetic screen was designed to generate and identify mutations that, in combination with the *fnt1* deletion, lead to respiratory deficiency. Approximately 10,000 colo-

nies were screened, and eight recessive synthetic petite mutants were isolated. One mutant strain, s.p. 175, was transformed with a yeast genomic library, resulting in four colonies (of 6000 screened) that harbored plasmids complementing the synthetic petite phenotype. These plasmids were rescued and their inserts sequenced, identifying a region of chromosome XVI spanning nucleotides 547857–557733. This region contains only three complete ORFs: *AEP3*, *LSP1*, and *ULA1* (Saccharomyces Genome Database). Because *AEP3* was previously characterized as a mitochondrial protein (24), the *AEP3* open reading frame was subcloned into the *LEU2* pRS415 vector and transformed into s.p. 175 yeast harboring the *FMT1* gene on pRS416 (*URA3* vector). The resulting Ura⁺ Leu⁺ transformants were re-streaked onto YPEG/5-FOA plates to select cells that evicted the pRS416-*FMT1* vector and to test for growth on a non-fermentable carbon source (YPEG; YP + ethanol/glycerol). The growth of *AEP3*-expressing cells on YPEG/5-FOA demonstrates complementation of the s.p. 175 synthetic petite mutation (Fig. 1A). The *AEP3* locus was PCR-amplified from s.p. 175 genomic DNA. Sequence analysis revealed a single T-to-A point mutation that results in a tyrosine-to-asparagine substitution at amino acid 305 (Y305N). This point mutation alone (in a wild-type *FMT1* background) does not cause respiratory deficiency, whereas the null *aep3* mutant is unable to grow on the non-fermentable carbon source YPEG (Fig. 1B). The *aep3*-Y305N point mutation does, however, cause a slight growth deficit on YPEG, but not on YPD, which supports growth by fermentation (Fig. 1B).

It seemed likely that the genetic interaction between *FMT1* and *AEP3* was due to the lack of formylated mitochondrial Met-tRNA^{Met} in the *fnt1* mutant rather than some direct (physical) interaction between the proteins encoded by these two genes. If this is indeed the case, the Aep3p-Y305N mutant should be synthetically petite with any mutation that eliminates formy-

AEP3p Functions in Mitochondrial Translation Initiation

lated mitochondrial Met-tRNA_f^{Met}. The *MIS1* gene encodes the mitochondrial isozyme of trifunctional C₁-THF synthase, which is responsible for synthesis of mitochondrial 10-formyltetrahydrofolate (38). 10-Formyltetrahydrofolate is the formyl donor for the Met-tRNA formyltransferase (*FMT1* gene product) (39). Deletion of the *MIS1* gene eliminates the substrate for the formylation reaction, and *mis1* mutants contain only unformylated Met-tRNA_f^{Met} in their mitochondria (15). Thus, we tested whether the Aep3p-Y305N mutant exhibits a synthetic interaction with a *mis1* deletion. The s.p. 175/pRS416-FMT1 strain (*leu2 MIS1⁺ aep3-Y305N FMT1⁺*) was transformed with a PCR-amplified *LEU2* cassette with *MIS1*-flanking regions on each end of the *LEU2* gene to direct recombination at the *MIS1* locus. Genomic DNA was isolated from Leu⁺ transformants, and successful *mis1* gene disruption (*mis1::LEU2*) was verified by PCR (data not shown). Cells disrupted at the *MIS1* locus but still harboring the wild-type *FMT1* gene from the pRS416-FMT1 plasmid were unable to grow on YPEG plates (Fig. 1C), demonstrating a genetic interaction between *MIS1* and *AEP3*. This result confirms a role for Aep3p specifically in the initiation of mitochondrial protein synthesis in the absence of formylated initiator tRNA.

The genetic interaction between *AEP3* and *FMT1* (or *MIS1*) suggested that Aep3p might physically interact with factors that are involved in the initiation stage of mitochondrial protein synthesis. Mitochondrial IF2 is responsible for binding and delivering the initiator tRNA to the small ribosomal subunit, and the yeast mIF2 shows a 3–4-fold binding preference for formylated versus unformylated Met-tRNA_f^{Met} (8). We speculated that Aep3p might interact with ymIF2 to stabilize initiator tRNA binding. Alternatively, Aep3p might interact directly with the initiator tRNA. To distinguish these two possibilities, yeast Aep3p was purified for *in vitro* binding assays.

Expression of Aep3p as a Fusion Protein—Attempts to express in *E. coli* the yeast Aep3p fused to an N-terminal polyhistidine tag produced only insoluble protein (data not shown). Given the tight membrane association of Aep3p in yeast mitochondria (24), we constructed a MBP fusion in an attempt to increase its solubility (40). Therefore, the full-length *AEP3* ORF (606 amino acids) was cloned into the vector pMALc2H₁₀T to express N-terminal MBP and a decahistidine tag fused to Aep3p (MBP-Aep3). *E. coli* cells expressed this fusion protein at high levels in soluble form. MBP-Aep3 was purified by nickel affinity chromatography, resulting in nearly homogeneous preparation of fusion protein that migrated with an apparent mass of 110 kDa, consistent with the combined size of Aep3p plus MBP (Fig. 2). The MBP tag provides a useful handle in the pulldown assays described below. The Aep3p-Y305N mutant protein was also expressed as an MBP fusion, but the protein degraded rapidly (data not shown) and could not be used for *in vitro* assays.

Aep3p Does Not Exhibit Significant tRNA Binding—A filter binding assay was used to test whether Aep3p binds initiator tRNA. MBP-Aep3 exhibited no significant binding activity with either formylated or unformylated Met-tRNA_f^{Met} nor with Lys-tRNA^{Lys} (Fig. 3). Yeast mIF2 showed significant binding activity with unformylated Met-tRNA_f^{Met} (positive control). MBP alone showed no binding (negative control).

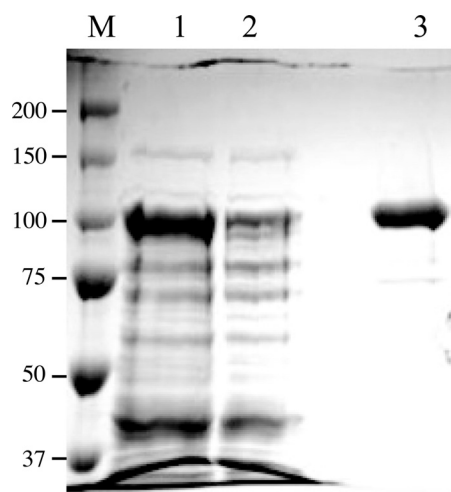


FIGURE 2. SDS-PAGE analysis of purification of MBP-Aep3p. Lane 1, soluble extract from induced cells. Lane 2, flow-through fraction from Ni²⁺ column. Lane 3, purified MBP-Aep3p (63 pmol). Sizes of molecular mass markers (M) in kDa are shown on the left. The 10% gel was stained with Coomassie Blue.

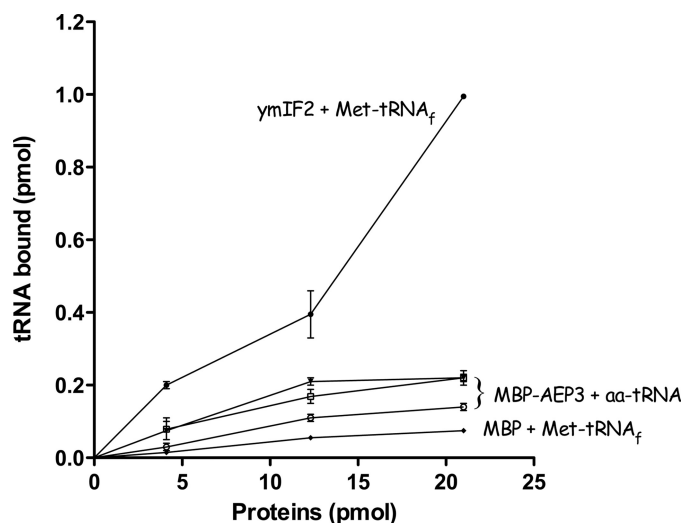


FIGURE 3. Aep3p exhibits no significant tRNA binding. Each reaction mixture contained the indicated amount of protein and 4 pmol of a labeled tRNA in the filter binding assay described under “Experimental Procedures.” MBP-Aep3p fusion protein was incubated with [³⁵S]Met-tRNA_f^{Met} (○), [³⁵S]Met-tRNA_f^{Met} (▼), or [¹⁴C]Lys-tRNA^{Lys} (□). ymIF2 + [³⁵S]Met-tRNA_f^{Met} (●) served as a positive control. MBP alone + [³⁵S]Met-tRNA_f^{Met} (◆) is a negative control. Nonspecific binding to the filters in the absence of protein was subtracted. Results shown are the means of two separate determinations ± S.E. (error bars are included for all data points but are obscured by the data symbol when the scatter is small).

Aep3p Interacts with ymIF2 in Vitro and in Vivo—We next used a MBP pulldown assay to test whether Aep3p physically interacts with ymIF2. Purified MBP-Aep3p and ymIF2 were incubated for 2 h at room temperature. Purified MBP alone was used as a control. Complexes were isolated with amylose affinity beads and analyzed by SDS-PAGE and immunoblotting with antibodies against ymIF2. Fig. 4 shows that ymIF2 (~70 kDa) is pulled down with MBP-Aep3p (lane 2) but not with MBP alone (lane 4). MBP-Aep3 also efficiently pulls down a 130-amino acid C-terminal fragment of ymIF2 (~16 kDa) (lane 6). This C-terminal segment contains the C2 subdomain, responsible for initiator tRNA binding (9). To rule out a nonspecific interaction due to Aep3p being a “sticky” protein (a common prob-

lem with membrane-associated proteins), we tested MBP-Aep3 with purified yeast cytoplasmic C₁-THF synthase (33). An immunoblot of the pulldown fraction with antibodies against C₁-THF synthase were negative (Fig. 4, lane 8), suggesting the interaction between Aep3p and ymIF2 is specific.

To test whether Aep3p binds ymIF2 *in vivo*, we prepared an HA-tagged version of Aep3p in a low-copy number vector (pRS415-AEP3-HA). This construct was transformed into a heterozygous diploid *aep3/AEP3* strain (Y22823; Table 1). The transformed strain was sporulated and dissected to obtain a haploid $\Delta aep3$ strain harboring pRS415-AEP3-HA. This strain grew normally on non-fermentable carbon sources (data not shown), confirming that the HA tag did not interfere

with AEP3 function. Extracts prepared from these cells were immunoprecipitated with antibodies against HA as described under "Experimental Procedures." However, immunoblots of the immunoprecipitates using antibodies against ymIF2 were negative (data not shown). In fact, using these antibodies we are unable to detect ymIF2 in whole cell extracts of *IFM1*⁺ yeast unless it is overexpressed from a plasmid (data not shown), suggesting that endogenous levels of ymIF2 are quite low. Therefore, we repeated the experiment using a strain co-expressing ymIF2 from a multicopy plasmid (pVT101U-ymIF2) and pRS415-AEP3-HA (low copy number). This strain (LOY1, Table 1) is disrupted at the chromosomal *IFM1* locus (encoding ymIF2) and expresses ymIF2 only from the plasmid. As shown in Fig. 5, anti-HA antibodies co-immunoprecipitated ymIF2 from extracts of the yeast strain expressing both AEP3-HA and ymIF2 (lane 2). No signal for ymIF2 was seen in an HA co-immunoprecipitate from an extract prepared from a strain lacking ymIF2 (lane 3). The diffuse immunostaining below 50 kDa in lanes 2 and 3 is a nonspecific cross-reaction of the anti-ymIF2 antibodies with additional proteins pulled down with the HA-tagged Aep3p. This cross-reaction is not observed in lane 1, as much less total protein is present in the immunoprecipitate due to lack of HA-tagged Aep3p in this control extract. Nonetheless, the 70-kDa ymIF2 band is clearly enriched in the HA-Aep3p pulldown assay (lane 2). These data suggest that the Aep3p-ymIF2 interaction observed *in vitro* also occurs *in vivo*.

Aep3p Stimulates the Binding of Unformylated Initiator tRNA to ymIF2—Our genetic and binding data suggest that Aep3p might interact with ymIF2 to stabilize initiator tRNA binding. The filter binding assay was used to test whether Aep3p affected the initiator tRNA binding by ymIF2 (Fig. 6). Seven pmol of ymIF2 were incubated with either formylated or unformylated Met-tRNA_f^{Met} and 0–21 pmol of MBP-Aep3. Under these conditions, in the absence of Aep3p, ymIF2 binds 2.7-fold more fMet-tRNA_f^{Met} than Met-tRNA_f^{Met}, as expected (8). MBP-Aep3 stimulated the binding of unformylated Met-tRNA_f^{Met} by ymIF2 in a dose-dependent fashion but had an inhibitory effect on the binding of formylated Met-tRNA_f^{Met} (Fig. 6).

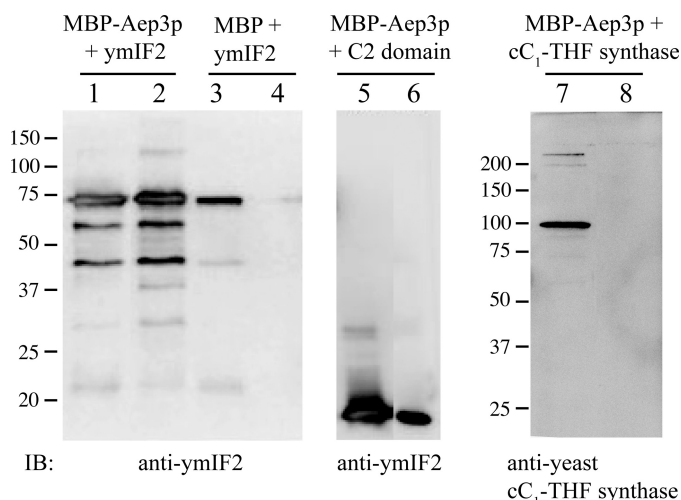


FIGURE 4. Aep3p binds ymIF2 *in vitro*. Purified proteins were incubated for 2 h at room temperature and treated with amylose beads as described under "Experimental Procedures." Unbound and bound fractions were analyzed by SDS-PAGE and immunoblotting (IB) with antibodies against ymIF2 (lanes 1–6) or cytoplasmic C₁-THF synthase (lanes 7–8). Lane 1, unbound fraction from MBP-Aep3p + ymIF2 incubation (40 pmol each); lane 2, bound fraction; lane 3, unbound fraction from MBP + ymIF2 incubation (20 pmol each); lane 4, bound fraction. Lane 5, unbound fraction from MBP-Aep3p + ymIF2 C2 domain incubation (20 pmol each); lane 6, bound fraction; lane 7, unbound fraction from MBP-Aep3p + cytosolic C₁-THF synthase incubation (20 pmol each); lane 8, bound fraction. Locations and size (kDa) of molecular mass markers are shown on the left of the gels.

TABLE 1
Yeast strains and plasmid constructs

	Relevant genotype	Source
Yeast strains		
Y03039	<i>MATa his3 leu2 met15 ura3 fnt1::KanMX4</i>	EUROSCARF
Y22823	<i>MATa/α his3/his3 leu2/leu2 lys2/LYS2 MET15/met15 ura3/ura3 aep3::KanMX4/AEP3</i>	EUROSCARF
DLY2 ^a	<i>MATα his3 leu2 met15 ura3 aep3::KanMX4</i>	This work
s.p. 175 ^b	<i>MATa his3 leu2 met15 ura3 fnt1::KanMX4 aep3-Y305N</i>	This work
LOY1	<i>MATα his3 leu2 lys2 ura3 ifm1::KanMX4</i>	Ref. 16
DAY4	<i>MATα ser1 leu2 trp1 ura3-52 his4</i>	Ref. 62
ATY6 ^b	<i>MATa his3 leu2 met15 ura3 fnt1::KanMX4 mis1::LEU2 aep3-Y305N</i>	This work
Plasmids		
pMALc2H ₁₀ T	His-tagged MBP fusion <i>E. coli</i> expression vector	Ref. 29
MBP-Aep3p	MBP-Aep3p fusion construct in pMALc2H ₁₀ T	This work
pRS416	Low-copy <i>URA3</i> yeast vector	Ref. 63
pRS415	Low-copy <i>LEU2</i> yeast vector	Ref. 63
pRS416-FMT1	Wild-type <i>FMT1</i> gene, including 360 bp of 5'-UTR, cloned into BamHI and ClaI sites of pRS416	This work
pRS415-AEP3	Wild-type <i>AEP3</i> gene, including 300 bp of 5'-UTR and 100 bp of 3'-UTR, cloned into BamHI and XhoI sites of pRS415	This work
pRS416-AEP3	Wild-type <i>AEP3</i> gene, including 300 bp of 5'-UTR and 100 bp of 3'-UTR, cloned into BamHI and XhoI sites of pRS416	This work
pRS415-aep3-Y305N	Y305N point mutant of <i>AEP3</i> gene, including 300 bp of 5'-UTR and 100 bp of 3'-UTR, cloned into BamHI and XhoI sites of pRS415	This work
pRS415-AEP3-HA	Wild-type <i>AEP3</i> gene, with C-terminal HA epitope tag, in pRS415	This work

^a Maintained with plasmid pRS416-AEP3 complementing the *aep3* deletion.

^b Maintained with plasmid pRS416-FMT1 complementing the *fnt1* deletion.

AEP3p Functions in Mitochondrial Translation Initiation

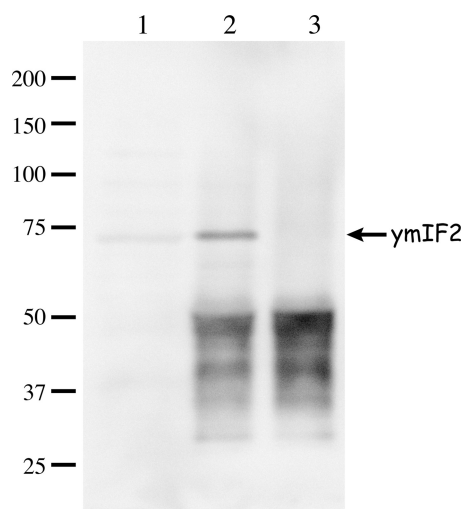


FIGURE 5. Aep3p binds ymIF2 *in vivo*. Yeast strain LOY1 ($\Delta ifm1$ AEP3) was grown in minimal medium containing glucose to $A_{600} = 3$, lysed, immunoprecipitated with anti-HA antibodies, and analyzed by SDS-PAGE and immunoblotting with antibodies against ymIF2 as described under "Experimental Procedures." Lane 1, control immunoprecipitate from cells harboring only wild-type *IFM1* multicopy plasmid pVT101U-ymIF2; lane 2, immunoprecipitate from cells harboring pVT101U-ymIF2 and HA-tagged AEP3 on plasmid pRS415-AEP3-HA; lane 3, immunoprecipitate from cells harboring only pRS415-AEP3-HA (no ymIF2). Locations and size (kDa) of molecular mass markers are shown on the left. ymIF2 migrates at ~ 70 kDa.

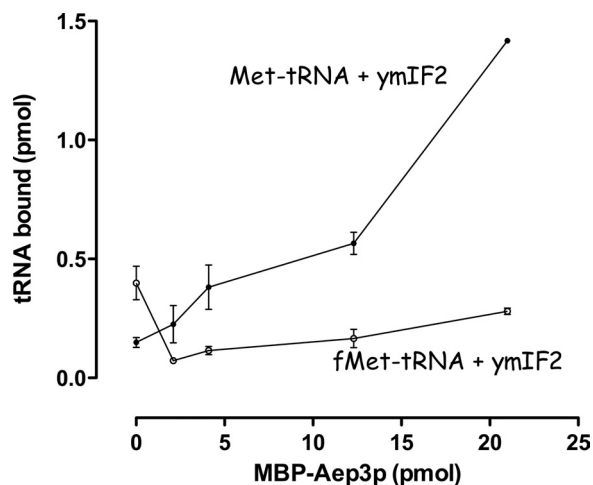


FIGURE 6. Aep3p stimulates the binding of Met-tRNA^{Met}, but not fMet-tRNA^{fMet}, to ymIF2. Each filter binding assay contained 7 pmol of ymIF2 and increasing amounts of MBP-Aep3p fusion protein with either 5 pmol of [³⁵S]Met-tRNA^{Met} (○) or 4 pmol of [³⁵S]fMet-tRNA^{fMet} (●). Nonspecific binding to the filters in the absence of protein was subtracted. Results shown are the means of two separate determinations \pm S.E. (error bars are included for all data points but are obscured by the data symbol when the scatter is small). At 0 MBP-Aep3p added, ymIF2 bound 0.15 ± 0.02 pmol of unformylated and 0.4 ± 0.07 pmol of formylated Met-tRNA^{Met}.

Aep3p-Y305N Causes a Mitochondrial Protein Synthesis Defect in Combination with $\Delta ifm1$ —The Y305N point mutant of AEP3 was identified as a petite mutation when combined with deletion of *FMT1*. To try to understand the cause of the petite phenotype, mitochondrial protein synthesis was analyzed in various AEP3/*FMT1* backgrounds. In an *FMT1*⁺ background, *aep3*-Y305N supported robust mitochondrial protein synthesis, including Atp6p (Fig. 7, lane 2) (our gel system does not resolve Atp8p from Atp9p, so we could not determine whether Atp8p was synthesized in the *aep3*-Y305N *FMT1*

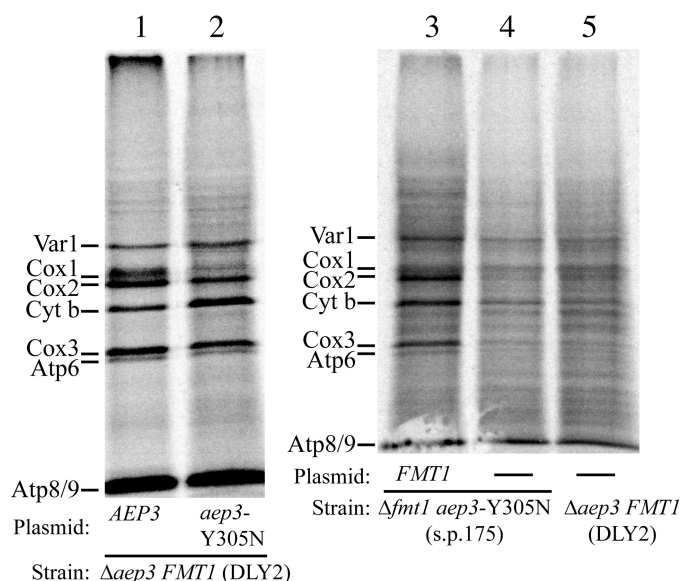


FIGURE 7. Aep3p-Y305N causes mitochondrial protein synthesis defect in combination with $\Delta ifm1$. Mitochondrially synthesized proteins were labeled *in vivo* with [³⁵S]methionine in the presence of cycloheximide, extracted, and analyzed by SDS-PAGE and phosphorimaging as described under "Experimental Procedures." Lanes 1 and 2, strain DLY2 ($\Delta aep3$ *FMT1*) harboring pRS415 plasmids with either wild-type AEP3 (lane 1) or point mutant *aep3*-Y305N (lane 2). Lanes 3 and 4, synthetic petite mutant strain 175 ($\Delta fmt1$ *aep3*-Y305N) harboring full-length *FMT1* on *URA3* plasmid (lane 3) or after eviction of *FMT1* plasmid (lane 4). Lane 5, strain DLY2 ($\Delta aep3$ *FMT1*) maintained with wild-type pRS416-AEP3, which was evicted by 5-FOA before metabolic labeling.

strain). Cox1 labeling appeared to be somewhat decreased compared with the AEP3 wild-type strain (Fig. 7, lane 1 versus 2). On the other hand, the *aep3*-Y305N point mutant causes a severe mitochondrial protein synthesis defect after *FMT1* is evicted (Fig. 7, lane 3 versus 4). Labeling of all the mitochondrial products is depressed, similar to that observed in the *aep3* deletion strain (Fig. 7, lane 5). We determined the percentage of petites in each population at the time of harvest for the protein synthesis assays using a tetrazolium overlay assay (15, 37). The strains represented in lanes 3–5 of Fig. 7 (*aep3*-Y305N *FMT1*, *aep3*-Y305N $\Delta ifm1$, $\Delta aep3$ *FMT1*) were 25, 80, and >99% petite, respectively. These results are consistent with the respiratory phenotypes observed in Fig. 1 and suggest that the petite phenotype of the $\Delta ifm1$ /*aep3*-Y305N genotype results from defective mitochondrial protein synthesis.

DISCUSSION

We demonstrate here a functional interaction between Aep3p and mitochondrial translation initiation factor 2, revealed when only unformylated initiator tRNA is available. A point mutant of the AEP3 gene, encoding a protein with a tyrosine-to-asparagine substitution at position 305, was found to cause a synthetic respiratory defect in cells lacking formylated Met-tRNA^{Met}. Aep3p was found to physically interact with mitochondrial IF2, and this interaction stimulated the binding of unformylated Met-tRNA^{Met} to ymIF2. We propose that Aep3p is an accessory initiation factor that stabilizes the mIF2-Met-tRNA^{Met} interaction in the 37 S initiation complex.

Aep3p was initially characterized as a mitochondrial inner membrane protein required for stabilization and/or processing

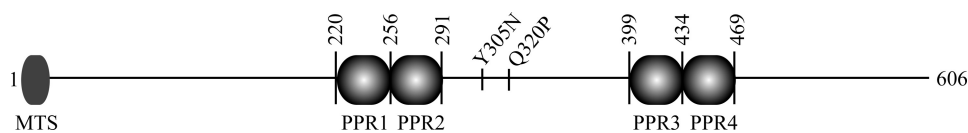


FIGURE 8. Predicted domain structure of Aep3p. The 606-amino acid AEP3 ORF was analyzed for PPR motifs using TPRpred (Bioinformatics Toolkit). The four highest scoring PPR motifs are indicated along with the residue numbers at their boundaries. The two point mutations discussed in the "Discussion" (Y305N, Q320P) are located in the region of highest sequence identity with Aep3p homologs in other related *Saccharomyces* species (46). MTS, mitochondrial targeting sequence.

of the bicistronic transcript of the mitochondrially encoded *ATP6/ATP8* genes (24). The *ATP6* and *ATP8* genes encode subunits of the mitochondrial ATP synthase. Deletion of the *AEP3* gene causes respiratory incompetence (petite phenotype) and reduces the levels of cytochromes *b* and *a + a3* as well as the activities of NADH-cytochrome *c* reductase, cytochrome *c* oxidase, and oligomycin-sensitive ATPase. *AEP3* deletion causes instability of the mitochondrial DNA, leading eventually to *rho*⁻/*rho*⁰ cells. Indeed, one of the hallmarks of *S. cerevisiae* strains impaired in mitochondrial protein synthesis is extreme instability of the mitochondrial DNA, giving rise to *rho*⁻ and *rho*⁰ mutants at high frequency (41). *In vivo* labeling of mitochondrial translation products revealed that both subunits 6 (Atp6p) and 8 (Atp8p) were almost undetectable (24). Northern analysis showed that in the *aep3* deletion strain, the long *ATP8/6* transcript was reduced to 34% that of wild-type levels, and the short *ATP8/6* transcript was undetectable. Finally, Aep3p possesses one or more degenerate pentatricopeptide repeat (PPR) motifs, which are implicated in RNA binding (42). Based on these data, Ellis *et al.* (24) propose that Aep3p interacts with the *ATP6/8* mRNA at the matrix side of the mitochondrial inner membrane, stabilizing the transcript and facilitating insertion of newly translated Atp6p and Atp8p subunits into the membrane for assembly into the functional F₀ component of the ATP synthase.

Our data suggest an additional, more general, role for Aep3p in mitochondrial translation; that is, as an accessory initiation factor that interacts with mIF2. This general translation initiation function is compatible with Aep3p inner membrane localization and specific involvement in *ATP6/8* mRNA translation. Mitochondrial protein synthesis is known to occur on the matrix face of the inner membrane (43), where Aep3p is localized. Although Ellis *et al.* (24) noted the dramatic loss of *ATP6/8* expression, translation of nearly all of the mitochondrially encoded proteins was depressed in their *aep3* deletion strain. Our *in vivo* labeling results (Fig. 7) are qualitatively similar.

The *aep3*-Y305N point mutant, on the other hand, supports respiration (Fig. 1) and mitochondrial protein synthesis (including Atp6p; Fig. 7) as long as formylated Met-tRNA_f^{Met} is available. However, when formylation of the initiator tRNA is prevented (either by *fmt1* or *mis1* mutation), the Y305N point mutant can no longer support robust mitochondrial protein synthesis and is respiratory-incompetent (petite). Translation of most of the mitochondrially encoded proteins is severely depressed under these conditions (Fig. 7). Thus, we propose that the petite phenotype of the *aep3*-Y305N Δ *fmt1* strain is caused by defective mitochondrial protein synthesis.

Physical interaction between Aep3p and mIF2, the initiation factor responsible for binding initiator tRNA, provides a bio-

chemical mechanism underlying the genetic interaction. This interaction, which was also observed *in vivo*, somehow stabilizes the binding of unformylated Met-tRNA_f^{Met} to ymIF2 (Fig. 6). In contrast, Aep3p appears to have an inhibitory effect on the binding of formylated Met-tRNA_f^{Met} by ymIF2. The binary

interaction between IF2 and initiator tRNA, even with formylated Met-tRNA_f^{Met}, is inherently weak and may not represent a physiologically relevant complex. The ternary complex of initiator tRNA, IF2, and 30 S subunit is much more stable than any of the binary complexes alone (44, 45). Thus, Aep3p may have a different effect *in vivo* than in these *in vitro* binding experiments. Nonetheless, the stimulatory effect seen with unformylated Met-tRNA_f^{Met} indicates that the physical interaction between Aep3p and mIF2 has functional consequences.

These *in vitro* binding data fit nicely with previously published genetic and metabolic data (15, 16). Both mammalian and yeast mIF2 show a distinct preference for binding formylated Met-tRNA_f^{Met}, yet both of these proteins support translation initiation *in vivo* with unformylated Met-tRNA_f^{Met} (16). We propose that Aep3p is a normal component of the mitochondrial translation initiation complex. When mitochondria contain formylated initiator tRNA, the major role of Aep3p is in facilitating *ATP6/8* translation (24). However, under conditions where formylation of the initiator tRNA is prevented, *e.g.* when mitochondria are deficient of folates or one-carbon units, Aep3p has a critical role in stabilizing the otherwise weak binding of unformylated Met-tRNA_f^{Met} by mIF2.

The mechanistic details of this stabilizing effect remain to be determined. Initiator tRNA can bind to the 30 S subunit in the absence of IF2 (45), and in fact, mutant yeast completely lacking mIF2 retain the ability to synthesize low levels of some mitochondrially encoded proteins (16). The structure of the 30 S initiation complex from *Thermus thermophilus* reveals binding interactions between the tRNA and the 30 S subunit, the tRNA and IF2, and IF2 and the 30 S subunit (45). It is the cooperativity of these interactions that provides for stable binding of the IF2-fMet-tRNA_f^{Met} subcomplex to the 30 S subunit. Assuming a similar structure exists for the mitochondrial small subunit (37 S) initiation complex, Aep3p may contribute further stability through its interactions with mIF2.

We do not know how the Y305N point mutation leads to defective function of Aep3p. The mutation may destabilize the protein, as we were unable to purify full-length recombinant mutant protein either alone or as a MBP fusion protein. Nonetheless, the Y305N mutant protein is apparently able to fulfill its *ATP6/8* stabilizing role *in vivo* in an *FMT1*⁺ background, as mitochondrial protein synthesis appears normal (Fig. 7), with the possible exception of a reduction in Cox1p. The Y305N mutation occurs in a region of high sequence identity with Aep3p homologs in other related *Saccharomyces* species (Fig. 8) (46). This region lies between two pairs of degenerate PPR motifs. Another mutation in this same region, Q320P, causes an acetate growth defect (47). Because acetate utilization requires mitochondrial respiration, this is also consistent with a role for

Aep3p Functions in Mitochondrial Translation Initiation

Aep3p in mitochondrial protein synthesis. Ellis *et al.* (24) suggested that this region “may be important for some other conserved function of Aep3p,” and it is tempting to speculate that this region is involved in the interaction with ymIF2.

It is likely that other mitochondrial translation initiation factors remain to be discovered. Vial *et al.* (48) showed that the phenotype of an *fnt1* disruption depends on the genetic background of the strain; growth on glycerol at a high temperature (37 °C) in rich medium or growth on glycerol in minimal medium at 30 °C was slower in some, but not all, Δ *fnt1* strains. This suggests that other gene products interact with the initiator tRNA in mitochondrial protein synthesis. In this context, Williams *et al.* (49) used a similar synthetic petite screen to search for genes that interact with RSM28, a dispensable component of the mitochondrial ribosomal small subunit. Their screen identified three interacting genes: *FMT1*, *IFM1*, and *RMD9*. The synthetic interaction between *FMT1* and *RSM28* reveals that initiator tRNA formylation is essential in the absence of Rsm28p. Thus, either the Y305N mutation in Aep3p (this work) or the loss of Rsm28p function (49) leads to a requirement for initiator tRNA formylation to support normal mitochondrial protein synthesis and respiratory growth. Genetic interaction with the genes encoding methionyl-tRNA formyltransferase and ymIF2 provides strong evidence that Rsm28p has a role in translation initiation. Williams *et al.* (49) speculate that the small subunit protein Rsm28p might provide IF1 and/or IF3-like functions in yeast mitochondrial translation initiation.

The other gene identified in their screen, *RMD9*, encodes an extrinsic membrane protein located on the matrix face of the mitochondrial inner membrane (50). *RMD9* was independently isolated as a high-copy suppressor of a respiratory-deficient *oxa1* mutant and was shown to control the processing and/or stability of several mitochondrial mRNAs (50). These data are consistent with the inner membrane localization of most of the mitochondrial gene expression machinery, including ribosomes (51, 52), translational activators (53), RNA processing and stability factors (24, 54, 55), and even RNA polymerase (54, 56). Nouet *et al.* (50) have proposed that Rmd9p delivers mRNAs to the inner membrane-localized ribosomes for translation and insertion of the nascent proteins into the membrane. The genetic interaction between *RMD9* and *RSM28* observed by Williams *et al.* (49) links Rmd9p function, like that of Aep3p, specifically with the initiation stage of translation.

Finally, it is worth noting that all four of the proteins in *S. cerevisiae* predicted to possess PPR motifs (Aep3p, Rmd9p, Pet309p, and Ccm1p) are mitochondrial proteins involved in the processing or stabilization of mitochondrial mRNAs (24, 50, 55, 57). Both Aep3p and Pet309p were initially discovered as factors that control the stability of a single mRNA (*ATP6/8* in the case of Aep3p; *COX1* in the case of Pet309p) (24, 58). However, the *COX1* and *ATP6/8* mRNAs are both derived from a single polycistronic *COX1-ATP6/8* transcript that is processed to yield the two mRNAs (24), so it might be expected that Aep3p and Pet309p function together. Tavares-Carreón *et al.* (59) showed that the PPR motifs in Pet309p are necessary for Cox1p translation but not for stabilization of the *COX1* mRNA. Rmd9p (50) and Ccm1p (57) appear to control the processing

and stability of multiple mitochondrial mRNAs. The function(s) of the PPR motifs shared by these four proteins are not known in any detail, but PPR motifs have been implicated in RNA binding and post-transcriptional gene regulation in organelles, including transcript processing and stabilization, tRNA binding, and translation (42, 60, 61). The discovery that Aep3p (this work) and Rmd9p (49) are also functionally linked to mitochondrial translation initiation factors suggests that the coupling between mRNA stability and translation may be a general phenomenon mediated by RNA-binding proteins and occurs mechanistically at the initiation stage.

Acknowledgments—We wish to acknowledge Dr. Theodor Hanekamp (1961–2004) for helping to design the genetic screen and Peter Ruymgaart for technical assistance.

REFERENCES

1. Gualerzi, C. O., and Pon, C. L. (1990) *Biochemistry* **29**, 5881–5889
2. Spremulli, L. L., Coursey, A., Navratil, T., and Hunter, S. E. (2004) *Prog. Nucleic Acid Res. Mol. Biol.* **77**, 211–261
3. Roll-Mecak, A., Cao, C., Dever, T. E., and Burley, S. K. (2000) *Cell* **103**, 781–792
4. Laalami, S., Sacerdot, C., Vachon, G., Mortensen, K., Sperling-Petersen, H. U., Cenatiempo, Y., and Grunberg-Manago, M. (1991) *Biochimie* **73**, 1557–1566
5. Gualerzi, C. O., Severini, M., Spurio, R., La Teana, A., and Pon, C. L. (1991) *J. Biol. Chem.* **266**, 16356–16362
6. Ma, J., and Spremulli, L. L. (1996) *J. Biol. Chem.* **271**, 5805–5811
7. Szkaradkiewicz, K., Zuleeg, T., Limmer, S., and Sprinzl, M. (2000) *Eur. J. Biochem.* **267**, 4290–4299
8. Garofalo, C., Trinko, R., Kramer, G., Appling, D. R., and Hardesty, B. (2003) *Arch. Biochem. Biophys.* **413**, 243–252
9. Garofalo, C., Kramer, G., and Appling, D. R. (2005) *Arch. Biochem. Biophys.* **439**, 113–120
10. Epler, J. L., Shugart, L. R., and Barnett, W. E. (1970) *Biochemistry* **9**, 3575–3579
11. Galper, J. B., and Darnell, J. E. (1969) *Biochem. Biophys. Res. Commun.* **34**, 205–214
12. Halbreich, A., and Rabinowitz, M. (1971) *Proc. Natl. Acad. Sci. U.S.A.* **68**, 294–298
13. Takeuchi, N., Kawakami, M., Omori, A., Ueda, T., Spremulli, L. L., and Watanabe, K. (1998) *J. Biol. Chem.* **273**, 15085–15090
14. Feldman, F., and Mahler, H. R. (1974) *J. Biol. Chem.* **249**, 3702–3709
15. Li, Y., Holmes, W. B., Appling, D. R., and RajBhandary, U. L. (2000) *J. Bacteriol.* **182**, 2886–2892
16. Tibbetts, A. S., Oesterlin, L., Chan, S. Y., Kramer, G., Hardesty, B., and Appling, D. R. (2003) *J. Biol. Chem.* **278**, 31774–31780
17. Laursen, B. S., Sørensen, H. P., Mortensen, K. K., and Sperling-Petersen, H. U. (2005) *Microbiol. Mol. Biol. Rev.* **69**, 101–123
18. Koc, E. C., and Spremulli, L. L. (2002) *J. Biol. Chem.* **277**, 35541–35549
19. Pearson, B. M., and Schweizer, M. (2002) *Yeast* **19**, 123–129
20. Allen, G. S., and Frank, J. (2007) *Mol. Microbiol.* **63**, 941–950
21. Gaur, R., Grasso, D., Datta, P. P., Krishna, P. D., Das, G., Spencer, A., Agrawal, R. K., Spremulli, L., and Varshney, U. (2008) *Mol. Cell* **29**, 180–190
22. Liao, H. X., and Spremulli, L. L. (1991) *J. Biol. Chem.* **266**, 20714–20719
23. Tzagoloff, A., and Dieckmann, C. L. (1990) *Microbiol. Rev.* **54**, 211–225
24. Ellis, T. P., Helfenbein, K. G., Tzagoloff, A., and Dieckmann, C. L. (2004) *J. Biol. Chem.* **279**, 15728–15733
25. Chan, S. Y., and Appling, D. R. (2003) *J. Biol. Chem.* **278**, 43051–43059
26. Kirksey, T. J., and Appling, D. R. (1996) *Arch. Biochem. Biophys.* **333**, 251–259
27. Gietz, R. D., and Woods, R. A. (2002) *Methods Enzymol.* **350**, 87–96
28. Robzyk, K., and Kassir, Y. (1992) *Nucleic Acids Res.* **20**, 3790

29. Kristelly, R., Gao, G., and Tesmer, J. J. (2004) *J. Biol. Chem.* **279**, 47352–47362
30. Bradford, M. M. (1976) *Anal. Biochem.* **72**, 248–254
31. Laemmli, U. K. (1970) *Nature* **227**, 680–685
32. Sundari, R. M., Stringer, E. A., Schulman, L. H., and Maitra, U. (1976) *J. Biol. Chem.* **251**, 3338–3345
33. Appling, D. R., and Rabinowitz, J. C. (1985) *J. Biol. Chem.* **260**, 1248–1256
34. Ray, P., Basu, U., Ray, A., Majumdar, R., Deng, H., and Maitra, U. (2008) *J. Biol. Chem.* **283**, 9681–9891
35. Sherman, F. (1991) *Methods Enzymol.* **194**, 3–21
36. Westermann, B., Herrmann, J. M., and Neupert, W. (2001) in *Mitochondria* (Pon, L. A., and Schon, E. A., eds) pp. 429–438, Academic Press, Inc., San Diego, CA
37. Ogur, M., St. John, R., and Nagai, S. (1957) *Science* **125**, 928–929
38. Shannon, K. W., and Rabinowitz, J. C. (1988) *J. Biol. Chem.* **263**, 7717–7725
39. Dickerman, H. W., Steers, E., Jr., Redfield, B. G., and Weissbach, H. (1967) *J. Biol. Chem.* **242**, 1522–1525
40. Kapust, R. B., and Waugh, D. S. (1999) *Protein Sci.* **8**, 1668–1674
41. Myers, A. M., Pape, L. K., and Tzagoloff, A. (1985) *EMBO J.* **4**, 2087–2092
42. Woodson, J. D., and Chory, J. (2008) *Nat. Rev. Genet.* **9**, 383–395
43. Pérez-Martínez, X., Funes, S., Camacho-Villasana, Y., Marjavaara, S., Tavares-Carreón, F., and Shingú-Vázquez, M. (2008) *Curr. Top. Med. Chem.* **8**, 1335–1350
44. Spencer, A. C., and Spemulli, L. L. (2005) *Biochim. Biophys. Acta* **1750**, 69–81
45. Simonetti, A., Marzi, S., Myasnikov, A. G., Fabbretti, A., Yusupov, M., Gualerzi, C. O., and Klaholz, B. P. (2008) *Nature* **455**, 416–420
46. Kellis, M., Patterson, N., Endrizzi, M., Birren, B., and Lander, E. S. (2003) *Nature* **423**, 241–254
47. Gresham, D., Ruderfer, D. M., Pratt, S. C., Schacherer, J., Dunham, M. J., Botstein, D., and Kruglyak, L. (2006) *Science* **311**, 1932–1936
48. Vial, L., Gomez, P., Panvert, M., Schmitt, E., Blanquet, S., and Mechulam, Y. (2003) *Biochemistry* **42**, 932–939
49. Williams, E. H., Butler, C. A., Bonnefoy, N., and Fox, T. D. (2007) *Genetics* **175**, 1117–1126
50. Nouet, C., Bourens, M., Hlavacek, O., Marsy, S., Lemaire, C., and Dujardin, G. (2007) *Genetics* **175**, 1105–1115
51. Szyrach, G., Ott, M., Bonnefoy, N., Neupert, W., and Herrmann, J. M. (2003) *EMBO J.* **22**, 6448–6457
52. Ott, M., Prestele, M., Bauerschmitt, H., Funes, S., Bonnefoy, N., and Herrmann, J. M. (2006) *EMBO J.* **25**, 1603–1610
53. Naithani, S., Saracco, S. A., Butler, C. A., and Fox, T. D. (2003) *Mol. Biol. Cell* **14**, 324–333
54. Rodeheffer, M. S., and Shadel, G. S. (2003) *J. Biol. Chem.* **278**, 18695–18701
55. Krause, K., Lopes de Souza, R., Roberts, D. G., and Dieckmann, C. L. (2004) *Mol. Biol. Cell* **15**, 2674–2683
56. Wang, Z., Cotney, J., and Shadel, G. S. (2007) *J. Biol. Chem.* **282**, 12610–12618
57. Moreno, J. I., Buie, K. S., Price, R. E., and Piva, M. A. (2009) *Curr. Genet.* **55**, 475–484
58. Manthey, G. M., and McEwen, J. E. (1995) *EMBO J.* **14**, 4031–4043
59. Tavares-Carreón, F., Camacho-Villasana, Y., Zamudio-Ochoa, A., Shingú-Vázquez, M., Torres-Larios, A., and Pérez-Martínez, X. (2008) *J. Biol. Chem.* **283**, 1472–1479
60. Davies, S. M., Rackham, O., Shearwood, A. M., Hamilton, K. L., Narsai, R., Whelan, J., and Filipovska, A. (2009) *FEBS Lett.* **583**, 1853–1858
61. Rackham, O., Davies, S. M., Shearwood, A. M., Hamilton, K. L., Whelan, J., and Filipovska, A. (2009) *Nucleic Acids Res.* **37**, 5859–5867
62. Tibbetts, A. S., and Appling, D. R. (2000) *J. Biol. Chem.* **275**, 20920–20927
63. Sikorski, R. S., and Hieter, P. (1989) *Genetics* **122**, 19–27